Supporting information

Regulating p-type conjugation in bipolar polyimide covalent organic frameworks for high-performance zinc dual-ion batteries

Suyu Qiu,[a] Decheng Zhao,[a] Tao Ye,[a] Hui Xu,[a] Lei Fang,[a] Mingxian Liu[a, b] and Liangchun Li*[a]

[a] *Key Lab of Chemical Assessment and Sustainability, School of Chemical Science and Engineering, Tongji University, 1239 Siping Road, Shanghai, 200092, China.*

[b] *State Key Laboratory of Cardiovascular Diseases and Medical Innovation Center, Shanghai East Hospital, School of Medicine, Tongji University, 150 Jimo Rd., Shanghai 200120, P. R. China*

*Corresponding author. E-mail: lilc@tongji.edu.cn

Table of Contents

1. General information

Powder X–ray diffraction patterns (PXRD). PXRD were recorded on a Bruker D8 Advance using Cu/*K*α radiation at 40 kV and 40 mA, from 2θ = 2° to 30° with 0.01° increment.

X–ray photoelectron spectroscopy (XPS). XPS characterization was carried out on a Thermo Scientific K–Alpha+ spectrometer. Monochromatic Al *K*α X–rays (1486.6 eV) were generated at operating voltage (12 kV) and filament current (6 mA) with photoelectrons collected from a 2-mm diameter analysis spot.

Fourier transform infrared spectroscopy (FT–IR). FT–IR spectra were recorded on a Thermo Nicolet IS20 FT–IR spectrometer from 4000 to 500 cm^{-1} using KBr pellets.

Scanning electron microscopy (SEM). SEM images were taken on a JSM–7900F (JEOL, Japan) with the field emission gun operating at an accelerating voltage of 3.0 kV.

Transmission electron microscopy (TEM). TEM images were obtained on a JEM–2100 (JEOL, Japan) microscope at an accelerating voltage of 200 kV. The samples were prepared by drop-casting sonicated ethanol

suspensions of the materials onto a copper grid.

Gas sorption analysis. Nitrogen sorption characterization was performed through a Micromeritics ASAP 2460 physisorption analyzer at the liquid nitrogen temperature of −196 °C to investigate the Brunauer–Emmett–Teller (BET) surface area and pore size distribution.

Computational details: Structural geometry optimization was carried out using BIOVIA Materials Studio suite of programs, using the Forcite module with the universal force field. Pawley refinement and simulation of the eclipsed AA-stacking mode were predicted using the Reflex module. The Pawley refinement was performed to optimize the lattice parameters iteratively until the R_{wp} and R_p value converged and the overlay observed with refined profiles showed good agreement.

All the density functional theory (DFT) calculations were performed with Gaussian 16 package. The structures of all the molecules were optimized by b3lyp/6–31g* functional, and the single-point energy calculations were based on b3lyp/6–311g** functional. The distribution of electrons and holes in the electron excitation process was calculated using Multiwfn (version 3.8).[S1] All figures were plot in Visual Molecule Dynamic 1.9.3 (VMD).[S2]

Gibbs free energies (ΔG) are defined as:

$$\Delta G = G_{\mathrm{COF-n\times ADSORBATE}} - G_{\mathrm{n\times ADSORBATE}} - G_{\mathrm{COF}}$$

where n = 0, 1, 2, 3..., and the value of n represents the number of bound adsorbate ions. The $G_{\mathrm{COF\text{-}n\times ADSORBATE}}$, $G_{\mathrm{n\times ADSORBATE}}$ and G_{COF} correspond to the Gibbs free energies of the adsorbate ions (Zn^{2+} or OTF^{-}) bind to the COFs, the isolated adsorbate and the pristine COFs, respectively.

Adsorption energy (ΔE_a) is defined as:

$$\Delta E_{\mathbf{a}} = [E_{\mathrm{TOTAL}} - (E_{ELECTRODE} + E_{\mathrm{ADSORBATE}})]$$

where E_{TOTAL} represents the total energy of system, and $E_{\mathrm{ELECTRODE}}$ and $E_{\mathrm{ADSORBATE}}$ are the total energies of the COFs and adsorbate (Zn^{2+} or OTF^{-}) in the solvent, respectively.

Electrochemical characterization: All electrochemical performances were examined at room temperature. The galvanostatic cycling performance tests were conducted on a Lanhe instrument at a voltage range of 0–1.8 V with different rates. CHI 760E electrochemical workstation (Shanghai, China) was used to carry out the cyclic voltammetry (CV) measurements at a scan rate of 1–10 mV s^{-1}, and the electrochemical impedance spectroscopy (EIS) tests with a voltage amplitude of 5 mV in the frequency range 0.1–10^5 Hz. The specific capacity was calculated based on the weight of COF loaded in the cathode electrode.

The charge storage kinetics of zinc batteries were investigated based on the following relationship: [S3]

$i = kv^b$

where k and b refer to constants, i and v are current density and scan rate, respectively. When the power exponent b value is close to 0.5, it identifies a diffusion-controlled process, while the b value close to 1.0 suggests a surface-dominated redox reaction process.

The Dunn's method was applied to analyze the capacitive contribution from the rapid surface redox capacitive process and the diffusion-limited process. Quantitative capacitive contribution can be calculated according to the following equation:

$i = k_1 v + k_2 v^{0.5}$

where k_1 and k_2 are constants, $k_1 v$ and $k_2 v^{0.5}$ are the current density contributed from fast capacitive process and diffusion-controlled process, respectively.

To fabricate organic cathodes, a mixture of PI-COF (120 mg, TPA-NDI or TPPA-NDI), acetylene black (60 mg), polytetrafluoroethylene (20 mg) was added into a solution of ethanol (100 mL). After the solvent evaporated, the electrode was divided into 32 equal parts with a 16-mm punch. The mass loading of COFs on the cathode is calculated to be 3 mg cm^{-2}. Then, organic cathodes were pressed onto the stainless-steel mesh and dried at 60 °C for 12 h under a vacuum condition. To construct

aqueous Zinc ion batteries (ZIBs), PI-COF (TPA-NDI or TPPA-NDI) cathode, 2 mol L^{-1} aqueous $Zn(CF_3SO_3)_2$ electrolyte (denoted as $Zn(OTF)_2$, 120 μL), Zn metal anode (> 99.99% purity), and glass fiber separator (Whatman) were packaged into 2032 coin-type cells.

Galvanostatic charge/discharge (GCD) curves and cyclic stability of batteries were tested on a LAND-CT-3004A battery test system. Cyclic voltammetry (CV) and electrochemical impedance spectroscopy (EIS) tests were performed on a CHI 660E electrochemical workstation. The specific capacity (C_m, mAh g^{-1}) was calculated from GCD curves based on the following equations:

$$C_m = \frac{I \times \Delta t}{m}$$

where I, Δt, m denote the current density (A g^{-1}), discharge time (s) and mass loading of active materials in cathodes, respectively.

The energy density (E, Wh kg^{-1}) and power density (P, W kg^{-1}) of ZIBs were calculated based on the following equations:

$$E = C_m \times \Delta V$$

$$P = \frac{3600 \times E}{\Delta t}$$

Where ΔV denotes the working voltage window. The electrochemical specific capacities and energy/power densities were estimated based on the mass loading of active organic materials in cathodes.

2. Material synthesis

TPA-NDI

According to the literature, TPA-NDI was prepared using optimized reaction conditions.[S4] 4,4',4''-nitrilotrianiline (14.5 mg, 0.05 mmol) and 1,4,5,8-naphthalenetetracarboxylic dianhydride (20.1 mg, 0.075 mmol) were added into a 10 mL pyrex tube. Then, a mixture of mesitylene (1.0 mL), 1,4-dioxane (1.0 mL), and isoquinoline (50 μL) was added. The pyrex tube was sealed after being evacuated under vacuum for three pump thaw cycles in a liquid nitrogen bath. After that, the sealed pyrex tube was placed in a vacuum oven at 200 °C for 3 days. The solid was isolated by centrifugation, washed with ethyl acetate, and further purified by Soxhlet extraction with tetrahydrofuran, methanol, and trichloromethane. The product was dried under vacuum at 50 °C for 12 h to give TPA-NDI (yield: 29 mg, 85%).

TPPA-NDI

According to the literature, TPPA-NDI was prepared using optimized reaction conditions.[S5] 4,4',4'',4'''-(1,4-phenylene)bis(nitrilo)tetrakisaniline (23.6 mg, 0.05 mmol) and 1,4,5,8-naphtha-lenetetracarboxylic dianhydride (26.8 mg, 0.10 mmol) were added into a 10 mL pyrex tube. And then, a mixture of mesitylene (1.0 mL), 1,4-dioxane (1.0 mL), and isoquinoline (50 μL) was added. The pyrex tube was sealed after being evacuated under vacuum for three pump thaw cycles in a liquid nitrogen bath. After that, the sealed Pyrex tube was placed in a vacuum oven at

200 °C for 3 days. The solid was isolated by centrifugation, washed with ethyl acetate, and further purified by Soxhlet extraction with tetrahydrofuran, methanol, and trichloromethane. The product was dried under vacuum at 50 °C for 12 h to give TPPA-NDI (yield: 40 mg, 81%).

3. Experimental data

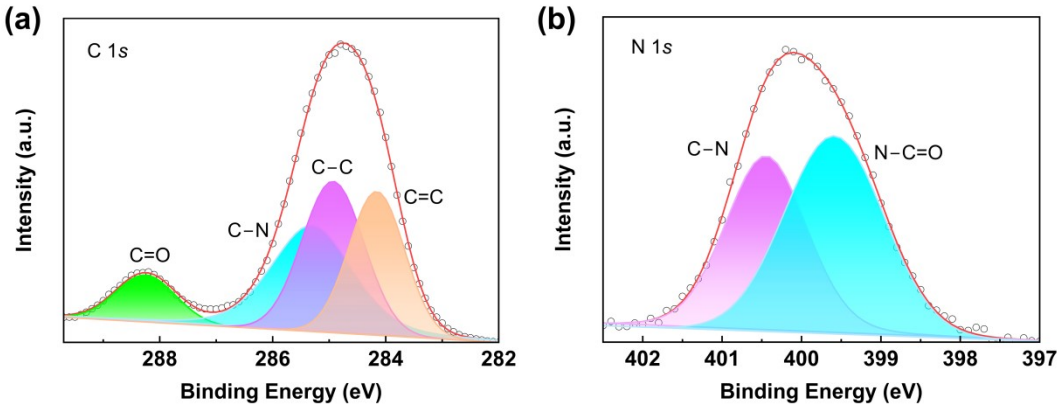

Fig. S1. XPS spectra (a) C 1*s* and (b) N 1*s* high-resolution spectrum of TPPA-NDI.

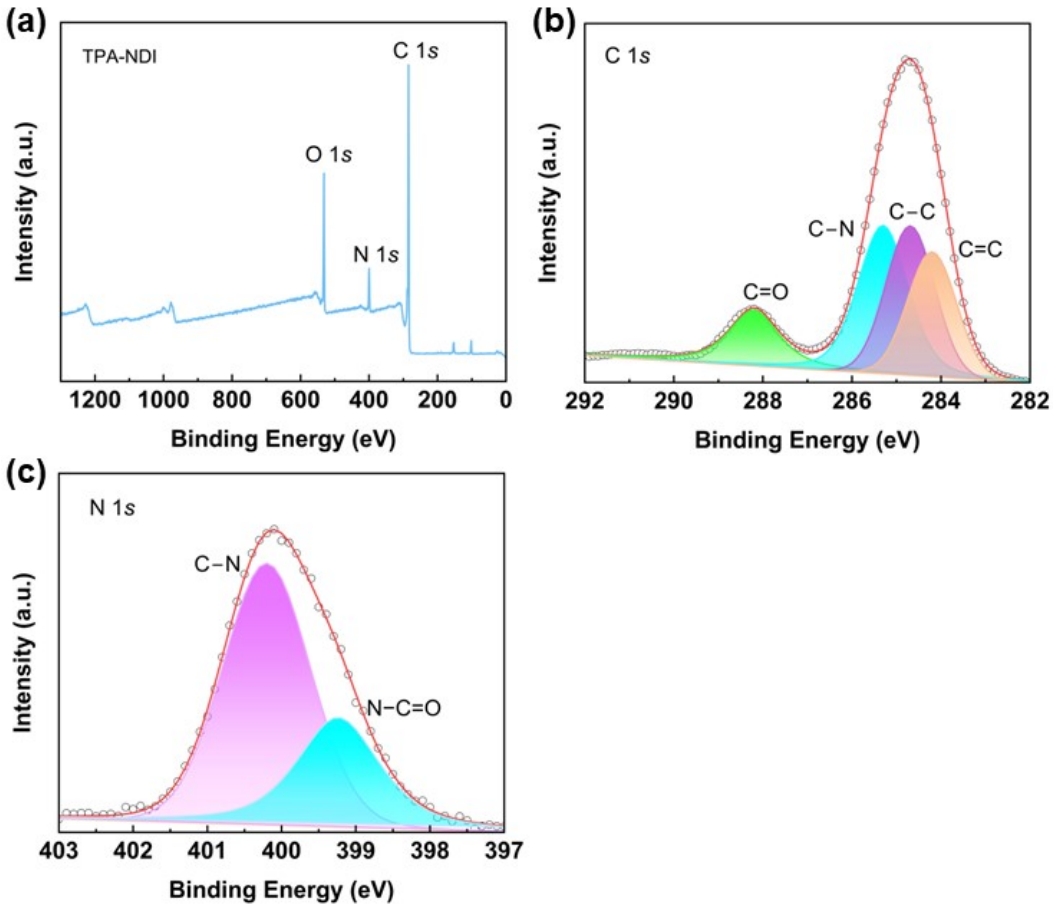

Fig. S2. XPS spectra (a) Full spectrum (b) C 1*s* and (c) N 1*s* high-resolution spectrum of TPA-NDI.

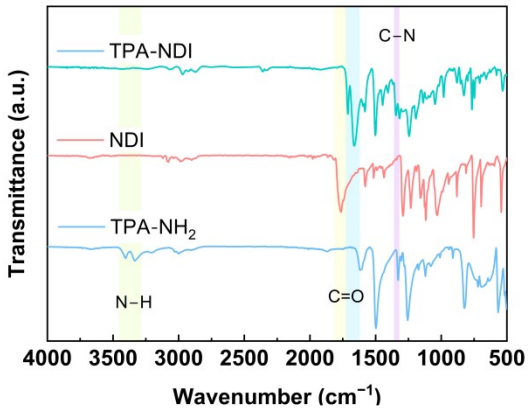

Fig. S3. FT–IR spectra of TPA-NDI.

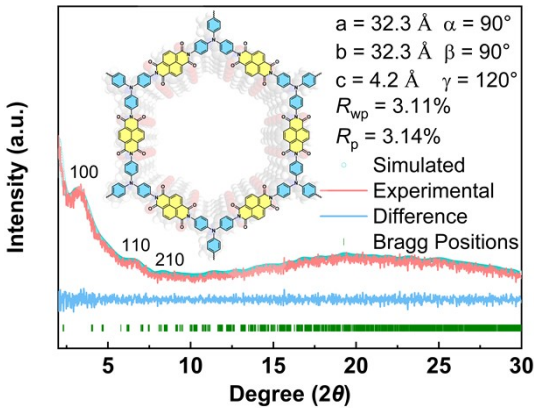

Fig. S4. PXRD data and simulated refinement of TPA-NDI.

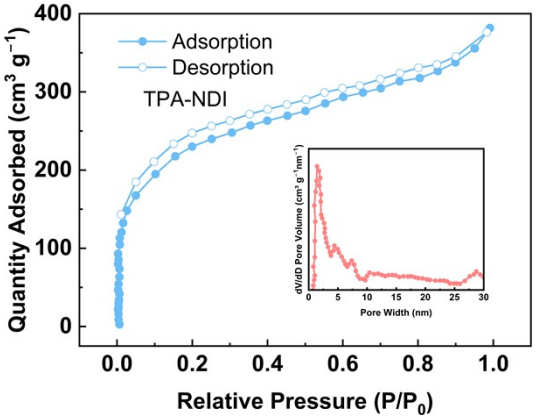

Fig. S5. N_2 adsorption–desorption isotherms of TPA-NDI (inset: pore size distribution).

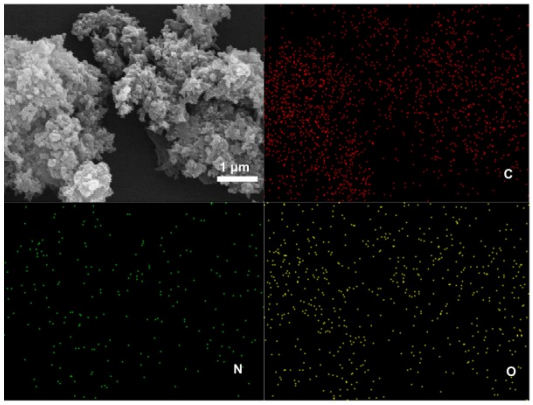

Fig. S6. Elemental mapping images of TPA-NDI.

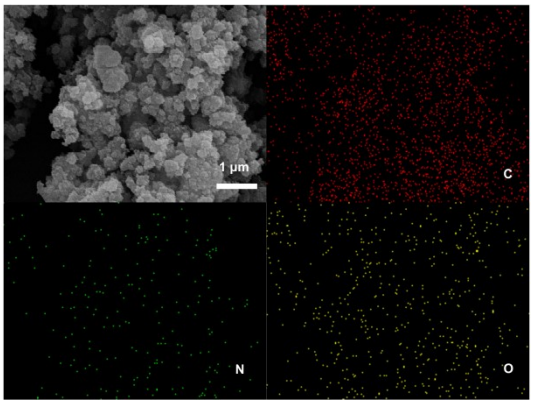

Fig. S7. Elemental mapping images of TPPA-NDI.

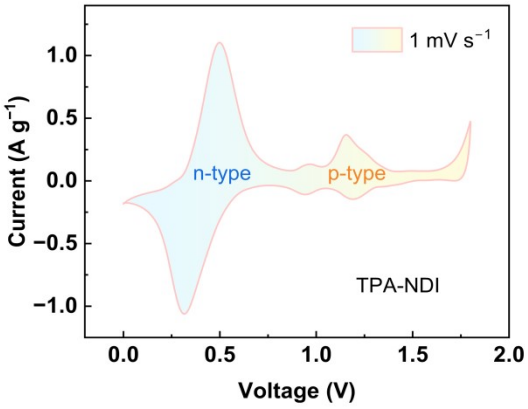

Fig. S8. CV curves of TPA-NDI at scan rate of 1 mV s^{-1}.

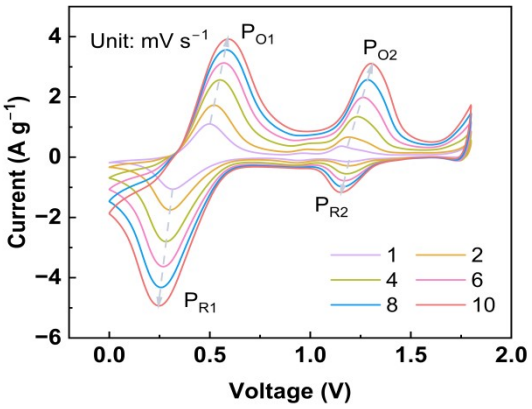

Fig. S9. CV curves of TPA-NDI at various scan rates.

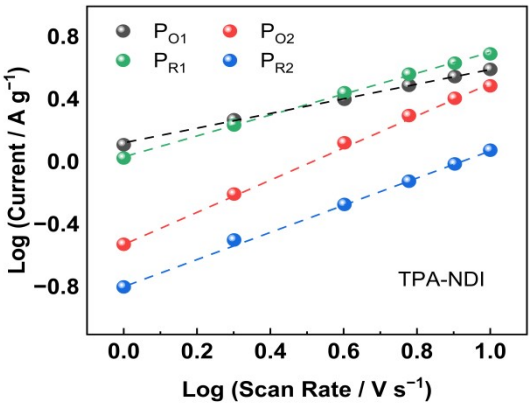

Fig. S10. The corresponding *b* value of TPA-NDI from the log (i)−log (v).

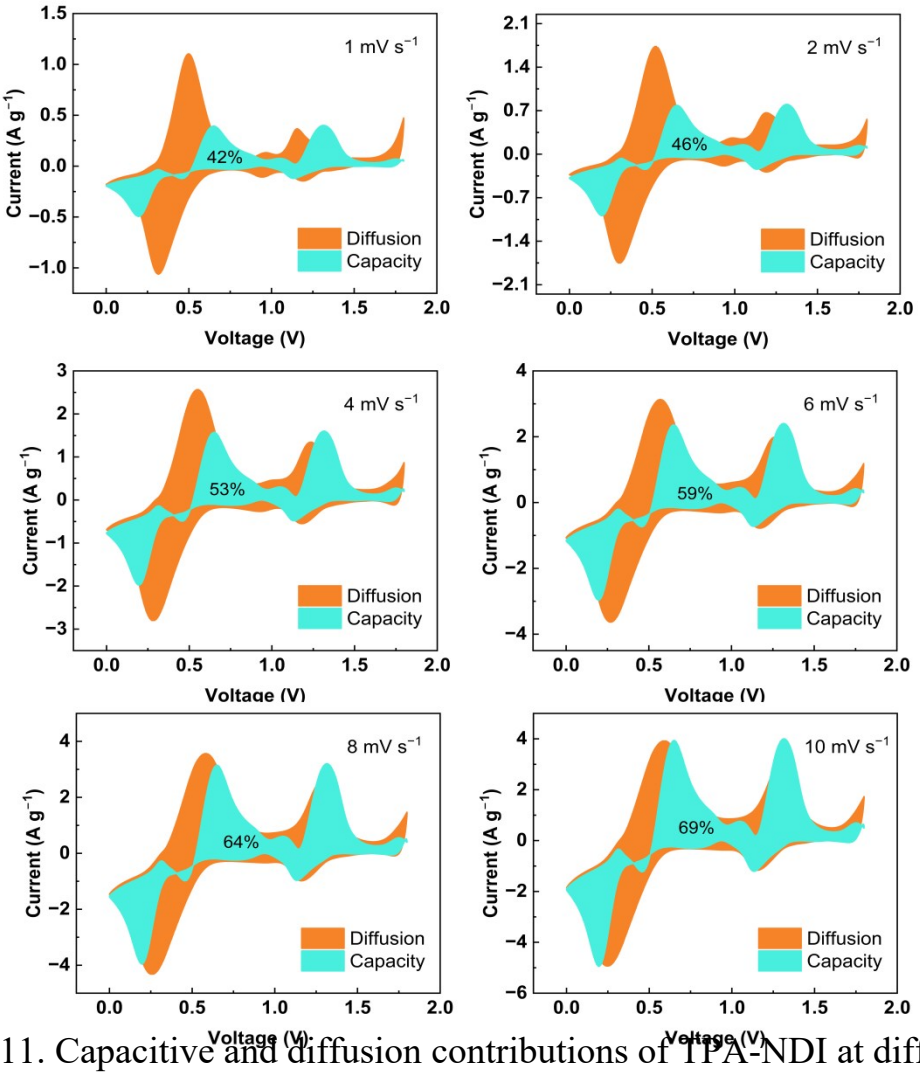

Fig. S11. Capacitive and diffusion contributions of TPA-NDI at different scan rates.

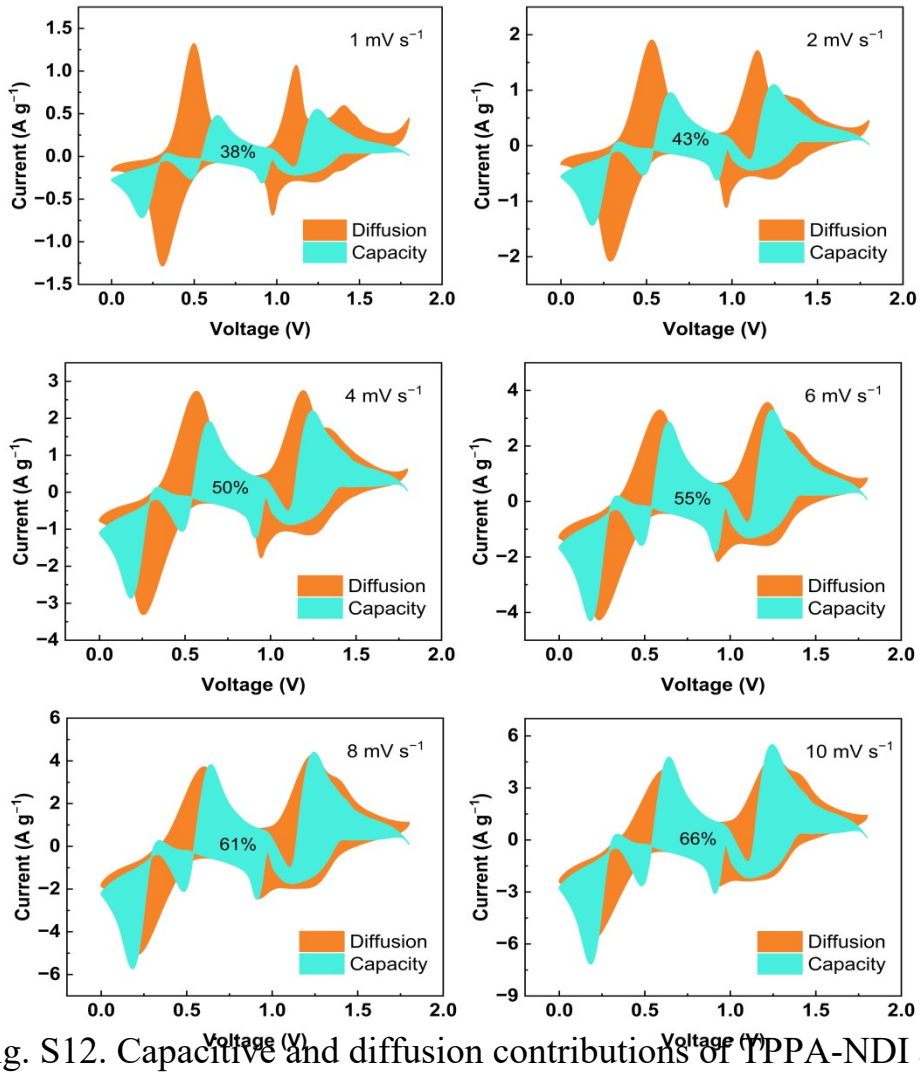

Fig. S12. Capacitive and diffusion contributions of TPPA-NDI at different scan rates.

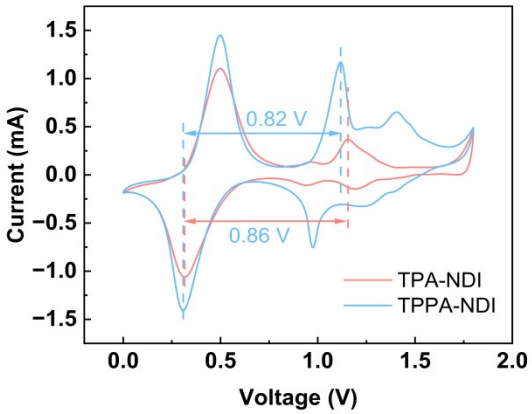

Fig. S13. CV curves of TPA-NDI and TPPA-NDI.

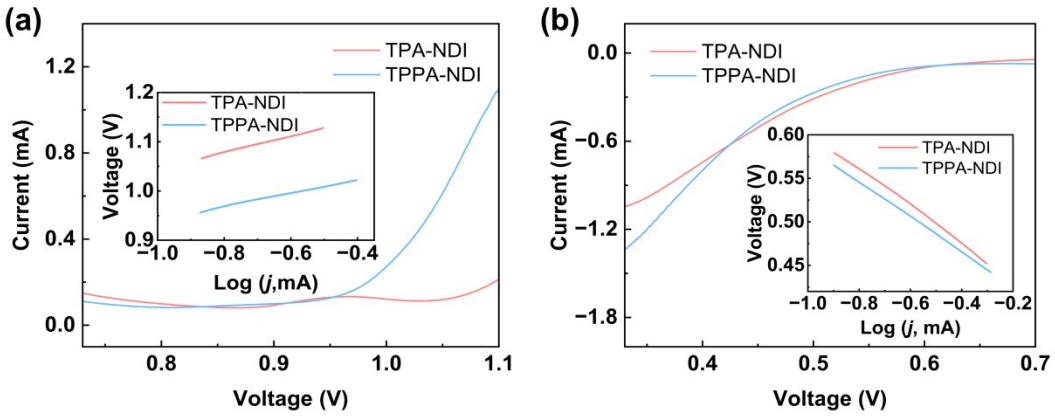

Fig. S14. (a–b) Linear sweep voltammetry curves obtained from Fig. S13 and the insets are the corresponding Tafel plots.

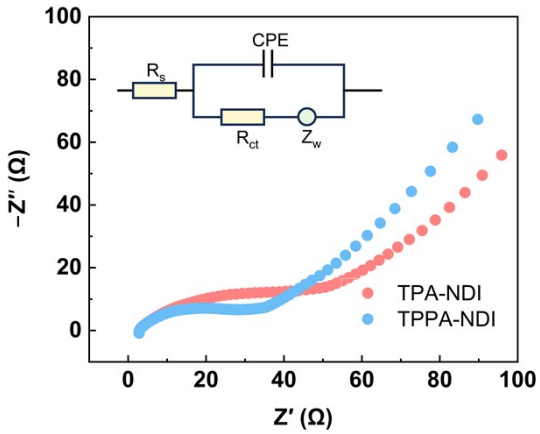

Fig. S15. Nyquist plots of TPA-NDI and TPPA-NDI.

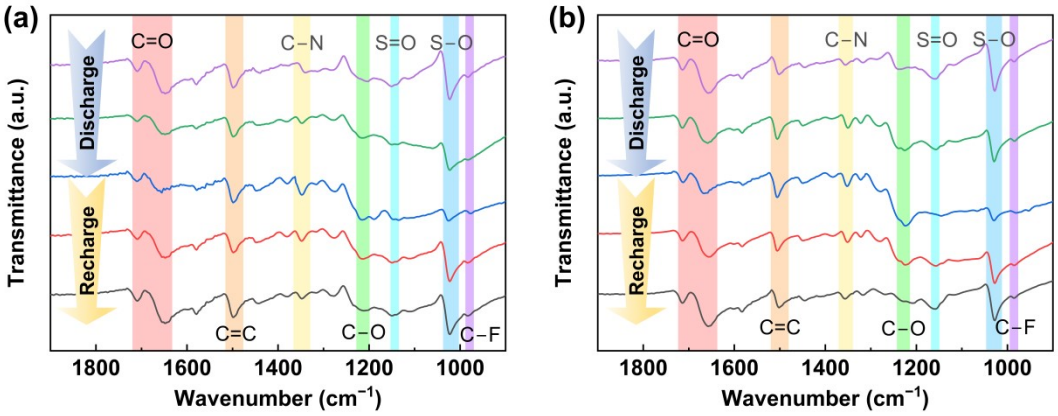

Fig. S16. Ex-situ FT–IR spectra of (a) TPPA-NDI and (b) TPA-NDI during charging and discharging processes.

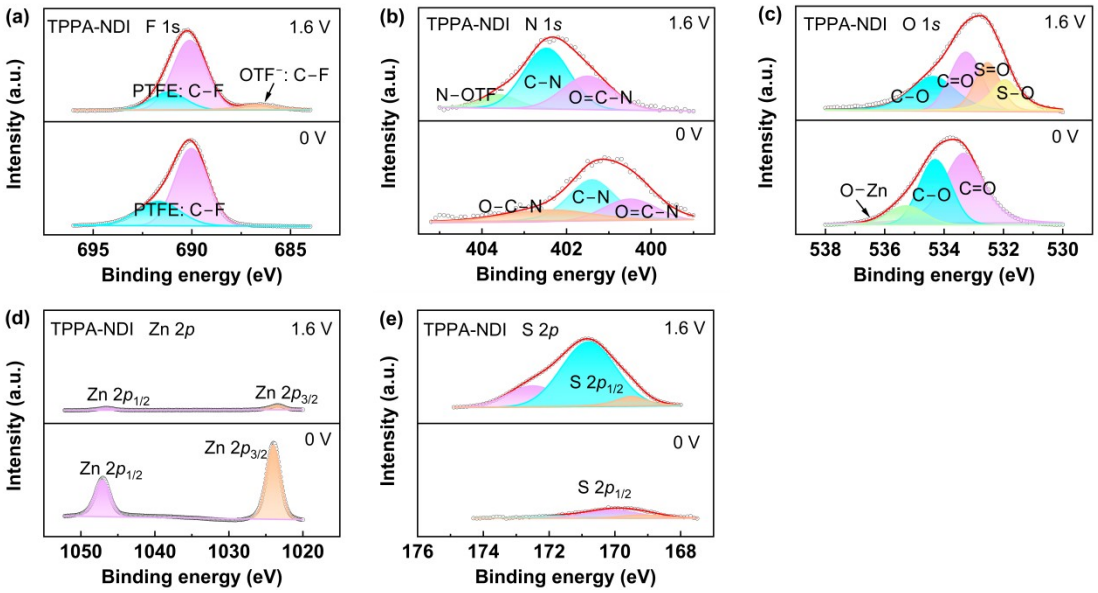

Fig. S17. (a–e) The XPS spectra of TPPA-NDI in charging and discharging states.

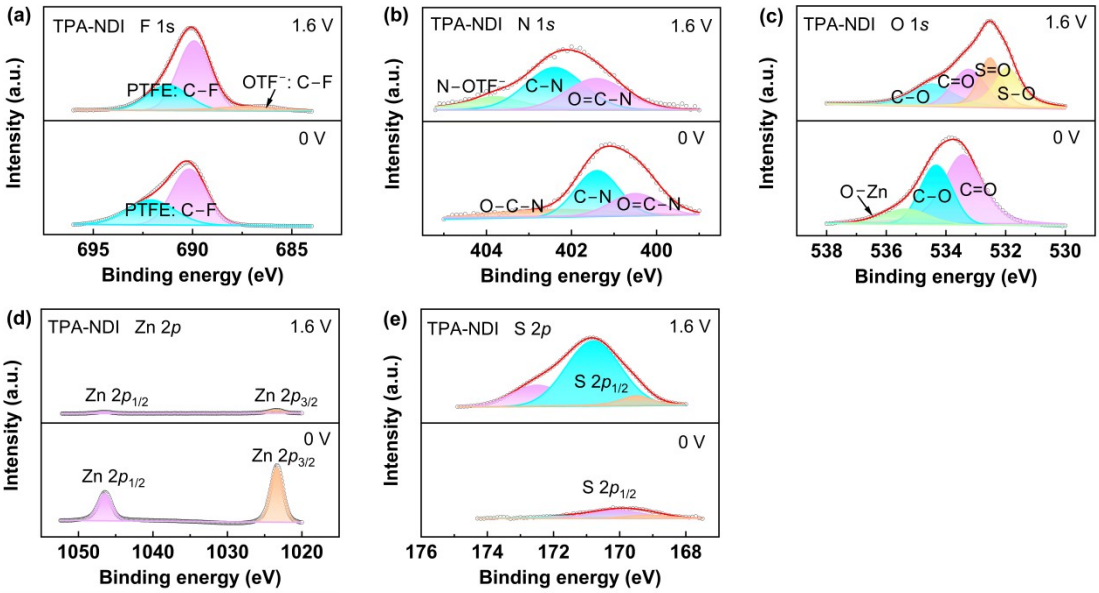

Fig. S18. (a–e) The XPS spectra of TPA-NDI in charging and discharging states.

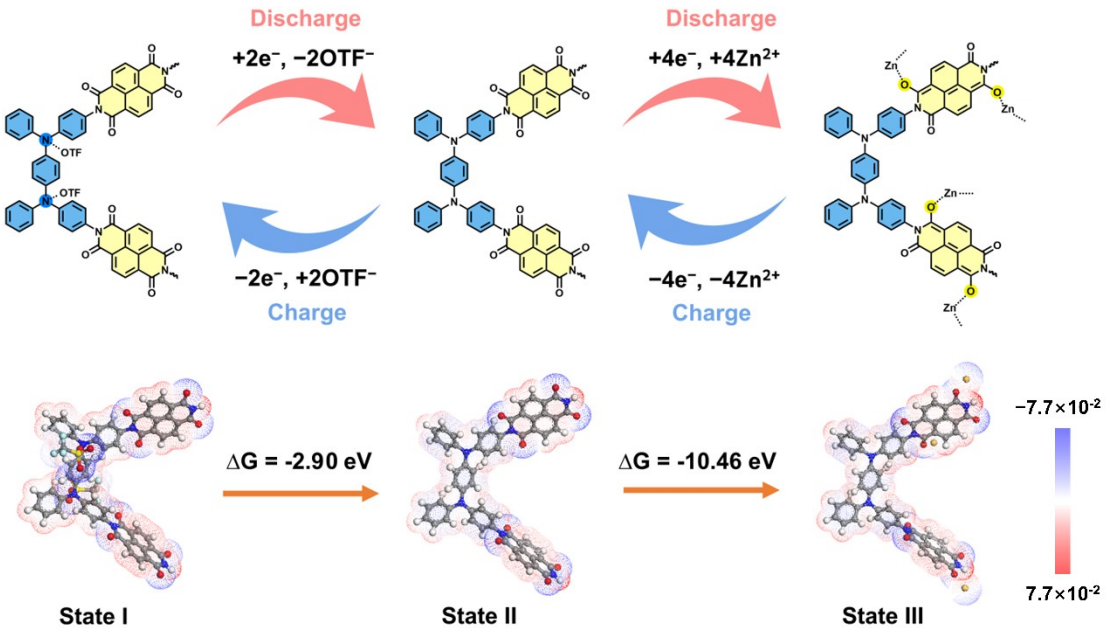

Fig. S19. The charge and discharge mechanism of TPPA-NDI.

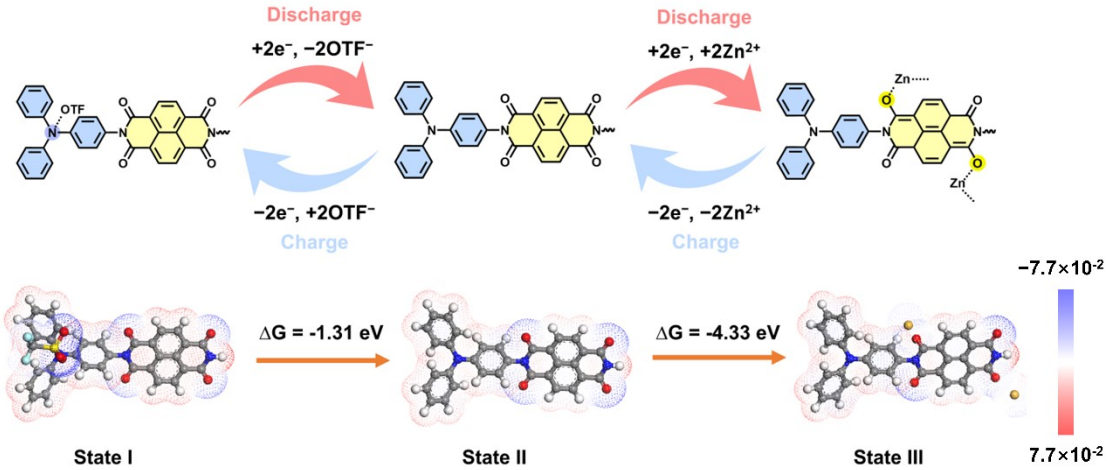

Fig. S20. The charge and discharge mechanism of TPA-NDI.

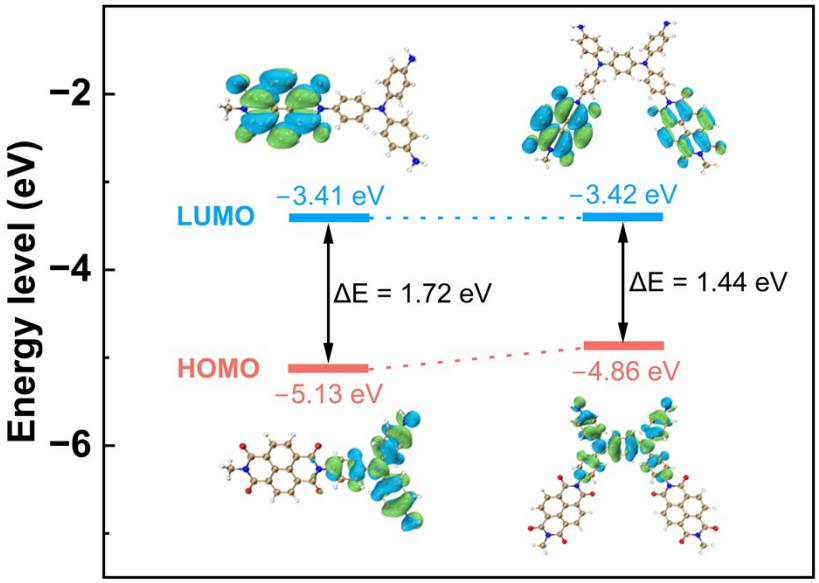

Fig. S21. LUMO/HOMO energy level diagram of TPA-NDI (left) and TPPA-NDI (right).

Table S1. Summary of electrochemical properties of zinc-ion batteries.

Charge carriers	Cathode	Anode	Electrolyte	Voltage window (V)	Cycling stability	Energy density (Wh kg^{-1})	Ref.
Zn^{2+}	PNZ	Zn	2 M $ZnSO_4$	~ 1.2	79.0%/1000/ 1 A g^{-1}	153	S6
Zn^{2+} and H^+	HATN-3CN	Zn	2 M $ZnSO_4$	~ 1	90.7%/5800/ 5 A g^{-1}	44.9	S7
Zn^{2+}	BT-PTO	Zn	3 M $Zn(OTF)_2$	~ 0.8	98.0%/10000/ 5 A g^{-1}	92.4	S8
Zn^{2+}	TMT-BT	Zn	2 M $Zn(OTF)_2$	~ 1	65.9%/2000/ 0.1 A g^{-1}	219.6	S9
Zn^{2+} and Cl^-	m-PTPA	Zn	2 M $ZnCl_2$	~ 1.1	87.6%/1000/ 6 A g^{-1}	236	S10
Zn^{2+} and OTF^-	TPPA-NDI	Zn	2 M $Zn(OTF)_2$	1.6	94.0%/5000/ 5 A g^{-1}	278.4	This work

Table S2. Fractional atomic coordinates for the unit cell of TPA-NDI.

C1	–0.54337	0.48638	0.68914	C68	0.86042	1.60796	0.53524
C2	–0.51819	0.46164	0.69146	C69	0.8353	1.62828	0.39226
C3	–0.47372	0.48006	0.53514	C70	0.78229	1.60155	0.39787
C4	–0.4553	0.52454	0.37882	C71	0.3329	1.14557	0.82406
C5	–0.48003	0.54971	0.38114	C72	0.30796	1.09567	0.8241
C6	–0.52441	0.53076	0.53514	C73	0.32764	1.07019	0.67823
N7	–0.44761	0.45395	0.53514	C74	0.37308	1.09531	0.53527
C8	–0.47372	0.40172	0.53515	C75	0.39339	1.07019	0.39234
C9	–0.39538	0.48006	0.53515	C76	0.43855	1.09567	0.24644
C10	–0.36933	0.52454	0.69146	C77	0.4635	1.14556	0.24641
C11	–0.31942	0.54971	0.68916	C78	0.91103	1.63327	0.53527
C12	–0.29399	0.53075	0.53517	C79	0.93615	1.61295	0.67824

C13	–0.31941	0.48637	0.38117	C80	0.91067	1.56779	0.82411
C14	–0.36932	0.46164	0.37884	C81	0.86078	1.54284	0.82408
C15	–0.51819	0.37567	0.37882	C82	0.86078	1.67344	0.24639
C16	–0.54337	0.32576	0.38115	C83	0.91067	1.69839	0.24642
C17	–0.52441	0.30034	0.53517	C84	0.93615	1.67871	0.39232
C18	–0.48003	0.32576	0.68918	C85	0.36666	1.01718	0.398
C19	–0.4553	0.37567	0.69148	N86	0.32171	0.99258	0.53532
C20	–0.60661	0.6787	0.67823	C87	0.30136	1.01718	0.67263
C21	–0.62693	0.63327	0.53525	C88	0.98916	1.63968	0.67263
C22	–0.60162	0.60796	0.53521	N89	1.01376	1.68463	0.53532
C23	–0.55618	0.62828	0.67815	C90	0.98916	1.70499	0.39799
C24	–0.5365	0.67344	0.82406	O91	0.38678	1.24582	0.79265
C25	–0.56145	0.69839	0.82409	O92	0.50987	1.24581	0.2777
C26	–0.62194	0.56253	0.39224	O93	1.01093	1.74477	0.27782
C27	–0.6671	0.54285	0.24637	O94	1.01092	1.62167	0.79282
C28	–0.69205	0.56779	0.2464	O95	0.26158	0.99542	0.79281
C29	–0.67237	0.61295	0.39231	O96	0.38468	0.99541	0.27785
C30	–0.63334	0.70498	0.67262	O97	0.76053	1.49647	0.79268
N31	–0.67829	0.68463	0.53531	O98	0.76053	1.61956	0.27768
C32	–0.69865	0.63968	0.39798	H99	–0.57765	0.47095	0.80851
C33	–0.5299	0.60155	0.67248	H100	–0.53411	0.42766	0.81159
N34	–0.55025	0.5566	0.53515	H101	–0.42131	0.54045	0.25869
C35	–0.59521	0.53625	0.39784	H102	–0.4646	0.584	0.26177
O36	–0.61533	0.74476	0.79281	H103	–0.38739	0.54046	0.81158
O37	–0.49012	0.61957	0.79264	H104	–0.30056	0.584	0.80853
O38	–0.61322	0.49647	0.27765	H105	–0.30056	0.47094	0.26181
O39	–0.73842	0.62166	0.27783	H106	–0.38739	0.42766	0.25872
C40	–0.74851	0.91547	0.38133	H107	–0.53411	0.39373	0.25868
C41	–0.77325	0.86556	0.37902	H108	–0.57765	0.3069	0.26178

C42	–0.75483	0.83951	0.53534	H109	–0.46461	0.3069	0.80856
C43	–0.71035	0.86556	0.69167	H110	–0.42132	0.39374	0.81162
C44	–0.68518	0.91547	0.68934	H111	–0.50176	0.68954	0.93857
C45	–0.70413	0.94089	0.53533	H112	–0.54535	0.73313	0.93863
N46	–0.78094	0.78728	0.53534	H113	–0.6832	0.5081	0.13183
C47	–0.83317	0.76117	0.53534	H114	–0.72679	0.55169	0.1319
C48	–0.75483	0.76117	0.53534	H115	–0.76394	0.93433	0.26195
C49	–0.77325	0.71669	0.69166	H116	–0.80723	0.8475	0.25889
C50	–0.74852	0.69152	0.68933	H117	–0.69444	0.8475	0.8118
C51	–0.70414	0.71048	0.53533	H118	–0.65089	0.93433	0.80871
C52	–0.68518	0.75486	0.38133	H119	–0.80723	0.70078	0.81179
C53	–0.71035	0.77959	0.37902	H120	–0.76394	0.65723	0.8087
C54	–0.85922	0.77959	0.69165	H121	–0.65089	0.77028	0.26196
C55	–0.90913	0.75486	0.68933	H122	–0.69444	0.81357	0.25889
C56	–0.93455	0.71048	0.53533	H123	–0.84116	0.81358	0.81178
C57	–0.90913	0.69152	0.38133	H124	–0.92799	0.77029	0.80869
C58	–0.85922	0.71669	0.37902	H125	–0.92799	0.65723	0.26196
N59	0.44974	1.24865	0.53518	H126	–0.84115	0.70078	0.25889
N60	0.75769	1.5566	0.53518	H127	0.31681	1.16421	0.93856
C61	0.4701	1.22405	0.39788	H128	0.27322	1.07703	0.93862
C62	0.44382	1.17104	0.39227	H129	0.45465	1.07702	0.13194
C63	0.39838	1.14592	0.53524	H130	0.49824	1.1642	0.13189
C64	0.37806	1.17104	0.67817	H131	0.92932	1.55169	0.93864
C65	0.40479	1.22405	0.6725	H132	0.84213	1.5081	0.93859
C66	0.78229	1.53624	0.67251	H133	0.84214	1.68954	0.13186
C67	0.8353	1.56252	0.67818	H134	0.92932	1.73313	0.13192

Table S3. Fractional atomic coordinates for the unit cell of TPPA-NDI.

C1	–1.59058	0.48399	–0.45397	C151	–1.65644	0.25109	–0.44461
C2	–1.56119	0.48861	–0.51517	C152	–1.68913	0.21831	–0.45348
C3	–1.52912	0.52171	–0.51793	C153	–1.68914	0.18587	–0.45322
C4	–1.52586	0.55081	–0.45975	C154	–1.59058	0.28368	–0.42879
C5	–1.55536	0.5462	–0.39878	C155	–1.55788	0.28334	–0.41879
C6	–1.58746	0.51312	–0.39623	C156	–1.55789	0.25089	–0.41514
N7	–1.62382	0.44996	–0.452	C157	–1.59061	0.21808	–0.42269
N8	–1.49249	0.58486	–0.46105	C158	–1.65604	0.28574	–0.44392
C9	–1.65824	0.44858	–0.45386	N159	–1.62348	0.31786	–0.43939
C10	–1.49319	0.61794	–0.45829	C160	–1.59097	0.31793	–0.43353
C11	–1.66708	0.464	–0.53658	C161	–1.65588	0.15134	–0.44216
C12	–1.70067	0.46252	–0.53846	N162	–1.62364	0.15131	–0.42835
C13	–1.7255	0.44629	–0.45638	C163	–1.59126	0.1833	–0.41819
C14	–1.71641	0.43091	–0.37348	O164	–1.68426	0.1231	–0.45481
C15	–1.68316	0.43172	–0.37298	O165	–1.68483	0.2856	–0.44624
C16	–1.51429	0.62417	–0.53004	O166	–1.56217	0.34625	–0.4336
C17	–1.51451	0.6565	–0.52831	O167	–1.56291	0.18321	–0.40367
C18	–1.49417	0.68285	–0.45379	C168	0.60544	1.08683	0.59556
C19	–1.47347	0.67626	–0.38096	C169	0.57301	1.05405	0.59854
C20	–1.47271	0.64425	–0.3841	C170	0.54182	1.04991	0.54766
C21	–1.49254	0.98286	–0.44543	C171	0.5441	1.07906	0.4918
C22	–1.51393	0.95586	–0.37376	C172	0.57645	1.11191	0.48966
C23	–1.51388	0.92344	–0.37319	N173	0.50773	1.01651	0.55477
C24	–1.4928	0.91723	–0.4455	C174	0.27545	0.91883	0.61694
C25	–1.47157	0.9442	–0.51759	C175	0.2769	0.94713	0.55869
C26	–1.47128	0.97678	–0.51724	C176	0.30922	0.9799	0.55155
C27	–1.88884	0.78046	–0.34374	C177	0.34072	0.98486	0.60207
C28	–1.85684	0.78328	–0.3844	C178	0.33903	0.95663	0.66176
C29	–1.82395	0.81661	–0.38175	C179	0.30667	0.92399	0.66922

C30	–1.82348	0.84703	–0.34006	C180	0.40828	1.01762	0.5811
C31	–1.85567	0.84394	–0.30018	C181	0.43963	1.04355	0.63214
C32	–1.88794	0.81099	–0.30152	C182	0.47208	1.04312	0.62381
C33	–1.79191	0.81923	–0.42153	C183	0.47391	1.01674	0.56402
C34	–1.79274	0.78862	–0.46299	C184	0.44252	0.99077	0.51303
C35	–1.82519	0.75584	–0.46607	C185	0.41005	0.99126	0.52131
C36	–1.85753	0.75298	–0.42759	H186	0.62915	1.08975	0.63608
C37	–1.78893	0.88186	–0.3395	H187	0.57203	1.03205	0.64214
N38	–1.7576	0.88446	–0.38005	H188	0.52061	1.0765	0.4509
C39	–1.75784	0.8545	–0.42023	H189	0.57766	1.13439	0.44816
C40	–1.92319	0.74548	–0.34944	H190	0.25302	0.94345	0.51752
N41	–1.92393	0.71586	–0.39296	H191	0.30986	1.00113	0.50464
C42	–1.89232	0.71847	–0.43051	H192	0.36299	0.9599	0.70157
O43	–1.9513	0.74387	–0.31926	H193	0.30589	0.90246	0.71536
O44	–1.78844	0.90829	–0.30288	H194	0.43886	1.06419	0.67835
O45	–1.73017	0.85696	–0.45673	H195	0.49591	1.06336	0.66433
O46	–1.89221	0.69175	–0.4632	H196	0.4432	0.97025	0.46595
C47	–1.86178	0.47693	–0.46765	H197	0.38617	0.9711	0.4807
C48	–1.8611	0.44509	–0.44864	H198	0.43665	0.46667	0.43804
C49	–1.82772	0.44526	–0.45201	H199	0.49306	0.52474	0.43343
C50	–1.79523	0.47742	–0.47091	H200	0.44666	0.5681	0.64781
C51	–1.79625	0.50905	–0.49009	H201	0.39024	0.51007	0.65179
C52	–1.82924	0.50874	–0.48908	H202	0.35192	0.47684	0.40025
C53	–1.82708	0.41332	–0.43579	H203	0.2927	0.4741	0.39617
C54	–1.85967	0.38151	–0.41445	H204	0.2651	0.41863	0.69129
C55	–1.89247	0.38151	–0.40872	H205	0.32348	0.41985	0.6916
C56	–1.89347	0.41324	–0.42559	H206	0.46992	0.60416	0.41201
C57	–1.76032	0.47749	–0.46921	H207	0.46966	0.66119	0.41427
N58	–1.7598	0.44586	–0.45622	H208	0.54211	0.69604	0.67792

C59	–1.79193	0.41381	–0.44194	H209	0.54352	0.63976	0.67231
C60	–1.897	0.47625	–0.46508	H210	0.4696	0.96016	0.68227
N61	–1.92866	0.44516	–0.43918	H211	0.46984	0.9031	0.68343
C62	–1.92806	0.41387	–0.41897	H212	0.54446	0.9398	0.42525
O63	–1.89777	0.50346	–0.48726	H213	0.54527	0.99724	0.42664
O64	–1.73195	0.50599	–0.47757	H214	0.14403	0.86705	0.73187
O65	–1.79173	0.38565	–0.43515	H215	0.08771	0.80948	0.72985
O66	–1.95597	0.38659	–0.39452	H216	0.23165	0.79003	0.50631
C67	–1.46035	0.84899	–0.44287	H217	0.17495	0.73275	0.50093
C68	–1.4935	0.81646	–0.44791	H218	0.22846	0.53407	0.49418
C69	–1.49372	0.78347	–0.44925	H219	0.17076	0.53349	0.49575
C70	–1.46078	0.78329	–0.4496	H220	0.14022	0.35657	0.59845
C71	–1.42782	0.81593	–0.44542	H221	0.08292	0.35665	0.60899
C72	–1.42761	0.84844	–0.4413	H222	0.59785	0.8163	0.55486
C73	–1.52683	0.75096	–0.45042	H223	0.59821	0.87318	0.56259
C74	–1.5596	0.75146	–0.45288	H224	0.41458	0.72663	0.54581
C75	–1.5594	0.784	–0.45426	H225	0.41491	0.78357	0.54298
C76	–1.52641	0.81671	–0.45165	H226	0.53017	0.5506	0.6669
C77	–1.46149	0.74854	–0.45541	H227	0.58875	0.55227	0.6607
N78	–1.49408	0.71652	–0.45246	H228	0.62005	0.62263	0.39454
C79	–1.52655	0.71662	–0.44821	H229	0.56202	0.62204	0.40399
C80	–1.46068	0.88326	–0.4385	H230	0.40804	0.42966	0.69291
N81	–1.49302	0.88349	–0.44581	H231	0.40708	0.37198	0.70038
C82	–1.5256	0.85154	–0.4537	H232	0.34611	0.33946	0.41341
O83	–1.43204	0.91134	–0.42759	H233	0.34548	0.39624	0.4094
O84	–1.43286	0.74854	–0.46408	H234	0.41259	0.07244	0.45617
O85	–1.55527	0.68844	–0.44151	H235	0.41293	0.12983	0.44708
O86	–1.55405	0.85176	–0.46395	H236	0.33945	0.0975	0.70792
C87	–1.45807	0.58609	–0.46424	H237	0.33822	0.03974	0.71517

C88	–1.6232	0.41691	–0.44929	H238	0.73617	0.17176	0.40435
C89	–1.4502	0.56645	–0.39233	H239	0.79226	0.22963	0.40918
C90	–1.41695	0.56733	–0.3962	H240	0.6522	0.24091	0.68974
C91	–1.39121	0.58757	–0.47307	H241	0.7083	0.29883	0.69414
C92	–1.39919	0.60727	–0.54485	H242	0.65241	0.4971	0.51687
C93	–1.43221	0.60683	–0.5398	H243	0.70981	0.49701	0.52003
C94	–1.6055	0.41002	–0.36818	H244	0.74404	0.67803	0.50671
C95	–1.60597	0.37735	–0.364	H245	0.80148	0.67799	0.4996
C96	–1.62341	0.35151	–0.44267	H246	0.28527	0.2178	0.53929
C97	–1.64068	0.35879	–0.52448	H247	0.28526	0.16104	0.53972
C98	–1.6409	0.39109	–0.52733	H248	0.46776	0.3082	0.58703
N99	–1.62535	0.01805	–0.40982	H249	0.46773	0.25146	0.59329
C100	–1.62491	0.05177	–0.41444	C250	0.85359	1.56651	0.46306
C101	–1.39281	0.11605	–0.45779	C251	0.88578	1.5658	0.47756
C102	–1.60365	0.07766	–0.48915	C252	0.91056	1.5869	0.55533
C103	–1.60332	0.11023	–0.4941	C253	0.90252	1.60881	0.61799
C104	–1.62395	0.1176	–0.42359	C254	0.87007	1.60901	0.60459
C105	–1.64488	0.09192	–0.34794	N255	0.94366	1.58581	0.57042
C106	–1.64551	0.05921	–0.34374	C256	0.97736	1.61897	0.57991
C107	–1.23008	0.25611	–0.49837	C257	0.94316	1.55193	0.57294
C108	–1.26139	0.252	–0.44869	C258	0.91406	1.52155	0.61958
C109	–1.29393	0.21844	–0.45117	C259	0.91317	1.48861	0.6209
C110	–1.29499	0.18931	–0.50442	C260	0.94127	1.48511	0.5744
C111	–1.26362	0.19384	–0.55426	C261	0.97086	1.51582	0.53047
C112	–1.23149	0.2269	–0.55146	C262	0.97182	1.5487	0.52983
C113	–1.32527	0.21425	–0.40134	N263	0.93976	1.45063	0.5715
C114	–1.32395	0.24357	–0.34918	C264	0.97269	1.44851	0.57022
C115	–1.29186	0.2767	–0.34672	C265	0.98906	1.63549	0.67729
C116	–1.26039	0.28121	–0.39628	C266	1.0215	1.66821	0.68631

C117	–1.32932	0.15434	–0.50656	C267	1.04376	1.68416	0.59837
N118	–1.35985	0.15036	–0.45641	C268	1.03215	1.66678	0.50136
C119	–1.35902	0.17883	–0.40411	C269	0.99891	1.63498	0.49186
C120	–1.1961	0.29123	–0.49423	C270	1.00247	1.47172	0.63244
N121	–1.19531	0.31974	–0.44241	C271	1.03441	1.47003	0.6318
C122	–1.22603	0.3162	–0.39436	C272	1.03754	1.4455	0.56662
O123	–1.16856	0.29468	–0.53449	C273	1.0079	1.42234	0.50387
O124	–1.33048	0.12913	–0.55367	C274	0.9757	1.42359	0.5064
O125	–1.38603	0.17486	–0.35878	C275	0.83829	1.35337	0.56331
O126	–1.22513	0.34188	–0.35115	C276	0.86527	1.3575	0.63357
C127	–1.15472	0.5879	–0.47289	C277	0.89848	1.3895	0.63664
C128	–1.25642	0.55487	–0.48489	C278	0.90517	1.41787	0.56925
C129	–1.2564	0.5875	–0.48943	C279	0.87798	1.41367	0.49907
C130	–1.28968	0.58754	–0.48785	C280	0.84476	1.3817	0.49615
C131	–1.32272	0.55491	–0.48607	H281	0.83495	1.55019	0.40247
C132	–1.32243	0.52247	–0.48455	H282	0.8915	1.54886	0.42794
C133	–1.28961	0.52246	–0.48294	H283	0.92104	1.6254	0.6784
C134	–1.28965	0.62022	–0.4872	H284	0.86405	1.62546	0.65532
C135	–1.25648	0.65263	–0.49252	H285	0.89173	1.52324	0.6543
C136	–1.22369	0.65257	–0.49678	H286	0.89059	1.46588	0.65882
C137	–1.22337	0.62009	–0.49459	H287	0.99327	1.51435	0.49612
C138	–1.35733	0.55545	–0.48538	H288	0.99474	1.57151	0.49383
N139	–1.3572	0.5876	–0.4793	H289	0.97251	1.6232	0.74585
C140	–1.32469	0.61977	–0.4791	H290	1.02984	1.6806	0.76241
C141	–1.22133	0.5554	–0.47862	H291	1.04849	1.67849	0.43216
N142	–1.18883	0.58751	–0.48408	H292	0.99007	1.62238	0.41615
C143	–1.18877	0.61951	–0.49579	H293	1.0008	1.49148	0.68037
O144	–1.22145	0.52718	–0.46648	H294	1.05695	1.48825	0.68048
O145	–1.38596	0.52713	–0.49152	H295	1.00984	1.40336	0.45305

O146	–1.32443	0.64814	–0.47019	H296	0.9534	1.40565	0.45666
O147	–1.16017	0.64761	–0.50782	H297	0.8604	1.33563	0.68497
C148	–1.65642	0.18551	–0.44322	H298	0.9191	1.39232	0.69144
C149	–1.62351	0.21813	–0.43393	H299	0.88283	1.43509	0.44562
C150	–1.62353	0.25105	–0.43572	H300	0.82424	1.3786	0.44066

Table S4. Total energy of TPA-NDI and TPPA-NDI from state I to state III.

	State I (Ha)	State II (Ha)	State III (Ha)
TAP-NDI	–733.4398	–1694.6369	–2201.4785
TPPA-NDI	–1234.8632	–3157.2678	–4171.0174

Table S5. The theoretically calculated value of the HOMO and LUMO for TPA-NDI and TPPA-NDI.

	LUMO (Ha)	HOMO (Ha)
TPA-NDI	–0.125240	–0.188489
TPPA-NDI	–0.125656	–0.178771

4. References

S1. T. Lu, F. Chen, *J. Comput. Chem.,* 2012, **33**, 580−592.

S2. W. Humphrey, A. Dalke, K. Schulten, *J. Mol. Graph. Model.,* 1996, **14**, 33−38.

S3. Z. Song, L. Miao, H. Duan, Y. Lv, L. Gan and M. Liu, *Angew. Chem. Int. Ed.*, 2024, **63**, e202401049.

S4. S. Wang, C. Zhu, J. Ji, M. Li, L. Zhao, F. Cai and Z. Tao, *Small Methods*, 2024, **8,** 2400557.

S5. S. Jindal, Z. Tian, A. Mallick, S. Kandambeth, C. Liu, P. M. Bhatt, X. Zhang, O. Shekhah, H. N. Alshareef and M. Eddaoudi, *Small*, 2024, **21,** 2407525.

S6. Q. Wang, Y. Liu and P. Chen, *J. Power Sources*, 2020, **468**, 228401.

S7. Z. Ye, S. Xie, Z. Cao, L. Wang, D. Xu, H. Zhang, J. Matz, P. Dong, H. Fang, J. Shen and M. Ye, *Energy Storage Mater.*, 2021, **37,** 378-386.

S8. S. Zheng, D. Shi, D. Yan, Q. Wang, T. Sun, T. Ma, L. Li, D. He, Z. Tao and J. Chen, , *Angew. Chem. Int. Ed.*, 2022, **61**, e202117511.

S9. H. Peng, S. Huang, V. Montes-García, D. Pakulski, H. Guo, F. Richard, X. Zhuang, P. Samorì and A. Ciesielski, *Angew. Chem. Int. Ed.*, 2023, **62**, e202216136.

S10. H. Zhang, L. Zhong, J. Xie, F. Yang, X. Liu and X. Lu, *Adv. Mater.*, 2021, **33**, 2101857.